

CEBAF PROPOSAL COVER SHEET

This Proposal must be mailed to:

CEBAF
Scientific Director's Office
12000 Jefferson Avenue
Newport News, VA 23606

and received on or before OCTOBER 31, 1989

A. TITLE: Deuteron Electrodisintegration at Threshold+at Large
Momentum Transfers

B. CONTACT PERSON: Jörg Jourdan

ADDRESS, PHONE
AND BITNET:

Dept. of Physics, Univ. Basel Klingelbergstrasse 82 4056 Basel Switzerland	41-61-321 2280 41-61-321 1440 (FAX) "JOURDAN%URZ.UNIBAS.CH@CERNVAX"
---	---

C. THIS PROPOSAL IS BASED ON A PREVIOUSLY SUBMITTED LETTER
OF INTENT

 M YES
 / NO

IF YES, TITLE OF PREVIOUSLY SUBMITTED LETTER OF INTENT

LOI's 88-02, 88-87

D. ATTACH A SEPARATE PAGE LISTING ALL COLLABORATION
MEMBERS AND THEIR INSTITUTIONS

=====
(CEBAF USE ONLY)

Proposal Received 11-6-89

Log Number Assigned PR-89-047

KES
contact: Jourdan

CEBAF Proposal

**DEUTERON ELECTRODISINTEGRATION AT
THRESHOLD AT LARGE MOMENTUM TRANSFERS**

J. Jourdan*, G. Masson, I. Sick
University of Basel, Basel, Switzerland

J. J. LeRose, J. Mougey*, S. K. Nanda, A. Saha, P. Ulmer
CEBAF, Newport News, VA

G. G. Petratos*
University of Rochester, Rochester, NY

P. E. Bosted, S. E. Rock
American University, Washington, D.C.

Z. E. Meziani
Stanford University, Stanford, CA

D. B. Day, R. W. Lourie, J. S. McCarthy, R. C. Minehart, O. Rondon Aramayo
University of Virginia, Charlottesville, VA

J. M. Finn, C. Perdrisat
College of William and Mary, Williamsburg, VA

* Spokespersons

ABSTRACT

We propose a single arm $d(e,e')$ experiment at electron energies up to 1.5 GeV in Hall A to extend the data for threshold electrodisintegration of the deuteron to the highest possible momentum transfer, limited by a cross section sensitivity of about $5 \times 10^{-42} \text{cm}^2 \text{sr}^{-1} \text{MeV}^{-1}$. In this region of momentum transfer the quark degrees of freedom are likely to be needed for a quantitative understanding, and one expects the threshold disintegration process to play as important a role in the study of non-nucleonic effects as it did at lower Q^2 in the study of mesonic degrees of freedom.

The excitation energy resolution will be 1 MeV, providing clear separation from the elastic scattering process. We request 600 hours of data taking at a current of 100 μA and 400 hours of check-out time at lower current.

1. MOTIVATION

Transverse electron-induced deuteron disintegration at threshold is an extremely important tool in the study of the nucleon-nucleon interaction and non-nucleonic degrees of freedom. It has been the subject of intense experimental and theoretical investigations and has provided some of the most striking evidence for the presence of meson-exchange currents (MEC) in the deuteron. The threshold inelastic scattering process is dominated by a spin-flip magnetic dipole transition from the isospin triplet $^3S_1 + ^3D_1$ ground state of the deuteron to the singlet state 1S_0 . This process produces a dramatic rise in the inelastic cross section at the breakup threshold ^[1-3] as can be seen in Figure 1.

Impulse approximation (IA) calculations exhibit a deep minimum in the cross section around $Q^2 = 12 \text{ fm}^{-2}$ due to the destructive interference between the $^3S_1 \rightarrow ^1S_0$ and $^3D_1 \rightarrow ^1S_0$ transitions. The experimental data from Saclay, ^[1] ^[8] plotted in Figure 2, depart strongly from the IA prediction around $Q^2 = 5 \text{ fm}^{-2}$, showing a smooth fall-off behavior up to $Q^2 = 28 \text{ fm}^{-2}$ and exceeding IA by several orders of magnitude around $Q^2 = 12 \text{ fm}^{-2}$. The Saclay cross sections are averaged over a region of energy loss extending from threshold breakup to a relative CM energy, E_{np} , of the np system of 3 MeV. The addition of pion-exchange currents ^[4-6] leads to an intriguingly good agreement with the data up to $Q^2 = 16 \text{ fm}^{-2}$. However, the IA contribution and the π -current contribution interfere destructively around $Q^2 = 25 \text{ fm}^{-2}$. In this region short-range properties such as ρ -meson exchange are needed to bring the theory in agreement with the data. Results of a typical calculation including ρ -currents and Δ isobar contributions (IC), performed by Mathiot ^[6] is shown in Figure 2.

However, above $Q^2 = 20 \text{ fm}^{-2}$, the interpretation of the data is not clear. The agreement obtained by Mathiot is very sensitive to the value assumed for the monopole cut-off mass Λ_π of the πNN off-shell vertex. Recent calculations based on a consistent derivation of the two body currents by Riska ^[7] and Buchmann *et. al.* ^[9] avoid the use of the *ad hoc* choice for the vertex form-factors by deriving

the exchange current operators directly from the nucleon-nucleon potential. The πNN and ρNN cut-off masses are implicitly included in the parametrization of the NN potential that is determined directly from nucleon-nucleon scattering data.

Though the latter approach removes some of the phenomenological arbitrariness, the whole picture remains complicated as the calculations show a sensitivity to the choice of NN potential and of nucleon isovector form-factors. The strong dependence of the cross section on the particular choice of nucleon-nucleon potential is demonstrated in the Singh *et. al.* calculations ^[9] as shown in Figure 3. It can be seen that otherwise identical calculations utilizing the Paris ^[10] and Bonn ^[11] potentials differ by a factor of two to five for $Q^2 > 10 \text{ fm}^{-2}$.

Most important is the question of whether mesonic and nucleonic degrees of freedom are sufficient for a quantitative understanding of the threshold electrodisintegration process at large momentum transfers, where the nucleonic substructure and dynamics are generally expected to make an increasing contribution and probably dominate. In recent years, several attempts have been made to simultaneously incorporate the quark- and gluon-exchange mechanism at short distance and the meson-exchange mechanism at long and intermediate distance in the electrodisintegration of the deuteron.

For example, Cheng and Kisslinger ^[12] have developed a hybrid quark-hadron model, in which the deuteron is divided into two distinct regions: an exterior one, described by baryon configurations and an interior one, described as the six-quark sector. When the internucleon separation is smaller than the matching radius $r_0 \sim 1 \text{ fm}$ of the two regions, the deuteron is treated as a six-quark configuration with a certain probability given by the overlap integral of the six quark wave function inside the matching radius. Glozman *et. al.* ^[13] treat the deuteron in a similar way but without the artificial separation of the nucleonic and six-quark configuration spaces. The results of calculations using these hybrid models are shown in Figure 4.

A more ambitious approach, followed by Yamauchi *et. al.*^[14] and Chemtob and Furui^[14], uses the resonating group method (RGM), where the two-baryon system is described as a composite of six equivalent quarks whose states are represented in terms of a three quark cluster basis and where the interaction mechanisms consist of quark-interchange effects, gluon-exchange perturbative corrections and pion-exchange effects. The calculations of the two RGM models are compared to the Saclay data in Figure 5.

All hybrid models are able to reproduce the existing Saclay data, but differ by up to 2 orders of magnitude above $Q^2=25 \text{ fm}^{-2}$. Although they are still in a phenomenological stage, they provide a basis for a quantitative description of the short distance (quark) structure of the deuteron and a bridge for treating short-range phenomena with a more fundamental QCD prediction.

An experiment at Bates^[14] plans to extend threshold electrodisintegration measurements up to 49 fm^{-2} and with a FWHM energy resolution of 1.6 MeV. The sensitivity limit of this experiment is a cross section measurement of about $5 \times 10^{-40} \text{ cm}^2/\text{sr}$ with 25% statistics. The experiment will run in early 1990 and requires a beam energy of 1 GeV.

Very recently, SLAC experiment NE4 measured threshold inelastic scattering with a FWHM energy resolution of 20 MeV. The experiment was primarily designed to measure the magnetic form factor of the deuteron. The threshold cross sections, averaged over a 10 MeV E_{np} bin, are shown in Figure 6.

The scope of this proposal is the measurement of the threshold deuteron disintegration with resolution comparable to the Saclay data and with a cross section sensitivity limit of about $5 \times 10^{-42} \text{ cm}^2/\text{sr}$. The experiment will provide a measurement of the $^3S_1 + ^3D_1 \rightarrow ^1S_0$ transition and the nearby threshold region of higher excitations. The results will put severe constraints on the diverging theoretical predictions at large momentum transfers and will lead to a better understanding of mesonic and quark-gluon degrees of freedom in the deuteron.

2. OVERVIEW OF THE EXPERIMENT

We propose to measure deuteron electrodisintegration at threshold to the highest possible Q^2 , limited to about 20% statistics in the 0 to 3 MeV E_{np} range, in a month of beam time with energy resolution of 1 MeV. The experiment will be performed in Hall A using the HRS electron spectrometer at a scattering angle of 160° . The large momentum acceptance of the spectrometer will allow measurement of the inelastic cross sections up to 100 MeV in E_{np} . The required beam energies will be from 0.5 to 1.5 GeV. A detailed kinematic list is given in Table 1.

The large scattering angle is chosen to minimize the contribution from the elastic electric form factor, $A(Q^2)$, and its radiative tail. The contribution of the tail to the integrated threshold inelastic cross section is shown in Figure 6. As compared to the NE4 integrated inelastic cross sections, the tail is many times smaller and should not be a limiting factor to the experiment.

The use of HRS is required for two reasons: a) the breakup threshold is separated by only 2.2 MeV from the elastic peak, requiring a momentum resolution better than 5×10^{-4} and b) the cross section for the breakup process are expected to be in the $10^{-39} - 10^{-42} \text{ cm}^2 \text{MeV}^{-1} \text{sr}^{-1}$ range, requiring a large solid angle.

To maximize the counting rate the experiment must use the longest possible target consistent with resolution requirements, the maximum beam current, and the maximum spectrometer acceptance. In this proposal we assume a beam current of $100 \mu\text{A}$ (half the accelerator design value) and a 15 cm long high-power liquid deuterium target, resulting in a luminosity of $4.8 \times 10^{38} \text{ cm}^{-2} \text{sec}^{-1}$.

To sufficiently separate threshold disintegration from elastic scattering, a FWHM resolution of about 1 MeV in excitation energy E^* ($E^* = W - M_d = E_{np} - E_b$, where W is the missing mass, M_d is the deuteron mass, and $E_b = 2.22 \text{ MeV}$ is the deuteron binding energy) is needed. The target length and cell construction have been optimized to achieve this resolution. The resolution will be dominated

by Landau straggling and multiple scattering in the target. Contributions from the beam energy spread and the spectrometer resolution are of minor concern. Analytic and Monte Carlo calculations have shown that the proposed experiment can achieve the desired resolution.

3. EXPERIMENTAL APPARATUS

3.1 TARGET

The experiment will require a cryogenic liquid deuterium target. Our calculations have shown that a length of 15 cm will be consistent with the resolution requirement. The power dissipated in the deuterium target (estimated to be 560 W) necessitates altering of the nominal parameters of the CEBAF beam. To prevent target density changes, the beam will have to be defocused horizontally to ~ 2 mm FWHM (a factor of 10 above the standard value) or alternatively be rastered over ~ 5 mm. The liquid will be circulated transversely to the beam direction at a flow rate of 1-1.5 m/sec. The predicted density change under these conditions will be less than 1%.^[18]

The contribution of the target walls to the resolution has been estimated assuming 0.051 mm thick Al. sidewalls and endcaps, plus 0.025 mm mylar superinsulation. Tungsten collimating slits will mask the spectrometer from the endcaps.

3.2 DETECTION SYSTEM

The detection system will consist of the standard drift chamber set for reconstruction of the kinematical coordinates of the scattered electron, two scintillation hodoscopes, and in addition, a gas threshold Čerenkov counter and a lead glass shower counter for particle identification. A combination of the information from the Čerenkov, the shower counter, and the timing between the hodoscopes will provide maximum background rejection.

To keep the event rate at a minimum level, the trigger logic will require either a coincidence among the Čerenkov counter, the hodoscope and a minimal shower energy, or a coincidence between the hodoscope and a large shower signal. This logic will also eliminate most of the cosmic ray background. The tight correlation of the position and angular divergence of the scattered electron in the drift chambers will reduce greatly the chances of misidentification of cosmic rays as events coming from the target. Adequate shielding of the detectors is needed to suppress the room background as much as possible.

4. EXCITATION ENERGY RESOLUTION—MONTE CARLO

The resolution in excitation energy ΔE^* is a function of the scattering angle Θ , the beam energy E and the scattered electron energy E' and their associated experimental uncertainties $\Delta\Theta$, ΔE , $\Delta E'$ and is given by:

$$\Delta E^* = \sqrt{\left(\frac{\partial E^*}{\partial E} \Delta E\right)^2 + \left(\frac{\partial E^*}{\partial E'} \Delta E'\right)^2 + \left(\frac{\partial E^*}{\partial \Theta} \Delta \Theta\right)^2}$$

where

$$\frac{\partial E^*}{\partial E} = \frac{M - 2E' \sin^2(\Theta/2)}{W} \simeq \frac{E'}{E}$$

$$\frac{\partial E^*}{\partial E'} = \frac{M + 2E \sin^2(\Theta/2)}{W} \simeq \frac{E}{E'}$$

$$\frac{\partial E^*}{\partial \Theta} = \frac{EE' \sin \Theta}{W} \simeq \frac{EE' \sin \Theta}{M_d}$$

The three partial derivatives which define the contribution of the $\Delta\Theta$, ΔE , $\Delta E'$ uncertainties are given together with the proposed kinematic settings in Table 1.

The beam energy uncertainty ΔE is due to ionization energy loss in the target endcap and deuterium. The excellent position resolution Δy_0 of HRS in the non-bend plane will allow reconstruction of the origin z_0 of the events in the target

and correct for the probable energy loss of the incident electrons. The correction will be limited by the Landau straggling and the Δz_0 uncertainty. The scattered energy uncertainty $\Delta E'$ is due to Landau straggling in the deuterium and the target exit wall. The probable energy loss in these two media is known and can be corrected for. The scattering angle uncertainty $\Delta \Theta$ is due to multiple scattering of the incident and backscattered electron in the deuterium liquid, the target entrance endcap and exit wall. The HRS angular and momentum resolutions make no sizable contribution to the overall ΔE^* .

It is clear that in order to obtain the best possible resolution, the deuterium target length and width must be minimized and that the target endcap and wall must have the minimum safe thickness. In addition to this, since the spectrometer angle is fixed, the target scattering chamber and the spectrometer vacuum pipe can be directly connected, eliminating vacuum windows.

The expected FWHM uncertainties in the incident and scattered electron energies and in the scattering angle as calculated using analytic formulas are given in Table 2 for the two extreme proposed kinematical settings. The calculations assume a 15 cm long deuterium target surrounded by 0.051 mm Al and 0.025 mm Mylar and a scattering angle of 160° . The total FWHM ΔE^* resolution and its separate components as a function of momentum transfer for $\Theta = 160^\circ$ are given in Table 3. The above calculations were verified by a Monte Carlo simulation program developed ^[19] for electron scattering experiments with HRS at CEBAF.

The Monte Carlo program simulated elastic electron deuteron scattering. It included the effects of energy loss and multiple scattering, ionization losses, and radiative energy losses. The program also simulated the angular and momentum resolutions of the spectrometer as well as the phase space of the incident and scattered electrons. The reconstructed elastic peak E^* distribution, which is a direct measure of the experimental resolution, is shown for the most extreme kinematics (worst case) of $Q^2 = 100 \text{ fm}^{-2}$ in Figure 7. The Figure shows successively the contribution of the different electron interaction effects to the

width of the elastic peak-resolution and the improvement of the z_0 reconstruction correction.

A typical separation of the threshold breakup from elastic scattering for this experiment is presented in Figure 8. The elastic peak from the Monte Carlo simulation and the theoretical calculation of Yamauchi *et. al.* of the threshold disintegration cross section convoluted with the expected excitation energy resolution are plotted for the proposed experimental conditions at $Q^2=70 \text{ fm}^{-2}$. The Figure demonstrates a clean separation between the elastic and threshold inelastic processes.

5. COMMITMENT OF COLLABORATORS

Naturally, all collaborators will participate in the actual set-up and data taking for the experiment. The CEBAF group will be deeply involved in the development of the HRS spectrometers in hall A. The College of William and Mary group will be involved in the design and development of detectors and the on-line data acquisition system. The University of Basel group intends to participate in the design and construction of a high-power liquid deuterium target. G. G. Petratos will run monte carlo simulations, help in the development of both the on-line and off-line analysis, and will participate in the calibration of the HRS. The American University and Stanford contributions will consist of assisting in the experimental set-up and on-line analysis.

7. SUMMARY

We propose to perform a high resolution measurement of the deuteron electrodisintegration at threshold and large momentum transfers. We will push the momentum transfer to the smallest possible count rate, which is expected to correspond to cross sections of the order of $5 \times 10^{-42} \text{ cm}^2\text{sr}^{-1}\text{MeV}^{-1}$. The facilities needed will be available in the early phase of the commissioning of the Accelerator and End Station.

In summary we request use of a) the Hall A facilities with the HRS spectrometer instrumented for electron identification, b) a liquid deuterium and hydrogen target, c) the Hall A data acquisition system and d) 550 hours of beam time for data taking and 450 hours for check-out and calibrations.

REFERENCES

- 1) M. Bernheim *et. al.*, Phys. Rev. Lett. **46**, 402 (1981).
- 2) B. Parker, Ph.D. Thesis, University of Massachusetts (1986).
- 3) S. Auffret *et. al.*, Phys. Rev. Lett. **55**, 1362 (1985).
- 4) J. Hockert *et. al.*, Nucl. Phys. **A217**, 14 (1973).
- 5) J. A. Lock and L. L. Foldy, Ann. Phys. (N.Y.) **93**, 276 (1975).
- 6) J. F. Mathiot, Nucl. Phys. **A412**, 201 (1984).
- 7) D. O. Riska, Phys. Scr. **31**, 107 (1985).
- 8) A. Buchmann *et. al.*, Nucl. Phys. **A443**, 726 (1985).
- 9) S. K. Singh *et. al.*, Z. Phys. **A331**, 509 (1988).
- 10) M. Lacombe *et. al.*, Phys. Rev. **C21**, 861 (1980).
- 11) R. Machleidt *et. al.*, Phys. Rep. **149**, 1 (1987).
- 12) T. S. Cheng and L. S. Kisslinger, Nucl. Phys. **A457**, 602 (1986).
- 13) L. Y. Glozman *et. al.*, Phys. Lett. **B200**, 406 (1988).
- 14) Y. Yamauchi *et. al.*, Phys. Letts. **B146**, 153 (1984).
- 15) M. Chemtob and S. Furui, Nucl. Phys. **A449**, 683 (1986).
- 16) R. Miskimen *et. al.*, Bates-MIT proposal (1987).
- 17) R. G. Arnold *et. al.*, SLAC-PUB-4918 (1989), submitted to PRL.
- 18) J. W. Mark, private communication.
- 19) G. G. Petratos, private communication.
- 20) H. Arenhövel, Prog. Th. Phys. Suppl. **91** (1987) 1
- 21) M. Gari and W. Krümpelman, Z. Phys. **A322**, 689 (1986)

TABLE CAPTIONS

1. The kinematics of the proposed experiment for different four momentum transfer settings. The three partial derivatives define the contribution of the beam energy E , the scattered electron energy E' and the scattering angle $\Theta = 160^\circ$ to the excitation energy resolution.
2. The expected FWHM resolutions of the incident energy E , the scattered electron energy E' and the scattering angle Θ under the proposed experimental conditions for the two extreme proposed kinematical settings.
3. The expected contributions to the E_{np} FWHM resolution from the incident energy E , the scattered electron energy E' and the scattering angle Θ under the proposed experimental conditions, versus four momentum transfer Q^2 . The three contributions added in quadrature yield the total resolution given in the last column.
4. Possible run plan and counting rates. The rates have been estimated using the 10 MeV averaged threshold cross sections of SLAC experiment NE4, for comparison cross sections and rates based on the calculations of Arenhövel^[20] are also shown. The cross sections and rate estimates are for a 3 MeV bin and assume a 15 cm liquid deuterium target, 100 μ A beam current, 8 msr spectrometer solid angle and a radiative correction factor of 0.7

TABLE 1
KINEMATICS

Q^2 (fm ⁻²)	E (GeV)	E' (GeV)	$\partial E_{np}/\partial E$	$\partial E_{np}/\partial E'$	$\partial E_{np}/\partial \Theta$ (MeV/mr)
20	0.56	0.35	0.632	1.583	0.037
30	0.73	0.41	0.571	1.751	0.055
40	0.87	0.46	0.525	1.904	0.073
50	1.01	0.49	0.488	2.049	0.092
60	1.15	0.52	0.457	2.187	0.110
70	1.28	0.55	0.431	2.321	0.128
80	1.40	0.57	0.408	2.451	0.146
90	1.53	0.59	0.388	2.578	0.165

TABLE 2
FWHM ENERGY – ANGULAR RESOLUTIONS

Q^2 (fm ⁻²)	30	90
<hr/>		
ΔE (MeV)		
Straggling in LD ₂	0.75	0.75
Straggling in Al ₂	0.01	0.01
Probable energy loss	0.15	0.15
TOTAL	0.76	0.76
<hr/>		
$\Delta E'$ (MeV)		
Straggling in LD ₂	0.29	0.29
Straggling in Al	0.02	0.02
Spectrometer resolution	0.07	0.10
TOTAL	0.30	0.31
<hr/>		
$\Delta \Theta$ (mr)		
Multiple scattering in LD ₂	3.9	2.6
Multiple scattering in Al	6.2	3.7
Spectrometer resolution	1.0	1.0
TOTAL	7.4	4.7
<hr/>		

TABLE 3
 E_{np} FWHM RESOLUTION

Q^2 (fm ⁻²)	Due to ΔE (MeV)	Due to $\Delta E'$ (MeV)	Due to $\Delta \Theta$ (MeV)	Total ΔE_{np} (MeV)
20	0.48	0.47	0.33	0.75
30	0.44	0.53	0.40	0.80
40	0.40	0.58	0.47	0.85
50	0.37	0.62	0.54	0.91
60	0.35	0.67	0.60	0.96
70	0.33	0.71	0.66	1.03
80	0.31	0.76	0.72	1.09
90	0.30	0.80	0.77	1.15

TABLE 4
RUN PLAN AND COUNTING RATES

$$\Theta = 160^\circ$$

$$\text{Target} = 15 \text{ cm LD}_2$$

$$\text{Current} = 100 \mu\text{A}$$

$$\Delta\Omega = 8 \text{ msr}$$

$$\text{Rad. Cor. factor} = 0.7$$

$$\Delta E_{np} = 3 \text{ MeV}$$

Q^2 (fm^{-2})	Cross section $\frac{\partial\sigma}{\partial E_{np}\partial\Omega}$ (fb/sr/MeV) (SLAC NE4 ^[17])	Rate (Counts/h)	Time (h)	Counts	Cross section $\frac{\partial\sigma}{\partial\omega\partial\Omega}$ (fb/sr/MeV) (Arenhövel ^[20])	rate (Counts)
20	35.0	459	3	1377	78	1794
30	3.89	51.1	11	562	1.6	35
40	1.44	18.9	18	346	0.19	2.5
50	0.53	7.0	30	207	0.10	1.2
60	0.20	2.6	49	125	0.036	0.40
70	0.072	0.95	83	79	0.014	0.14
80	0.027	0.35	140	49	0.0051	0.051
90	0.010	0.13	216	28		
Total			550			
Calibrations			150			
Check-out			300			
TOTAL			1000			

FIGURE CAPTIONS

1. Cross section for e-d scattering at $\Theta = 155^\circ$ and incident energies of 280 and 410 MeV ($Q^2 = 5.9$ and 11.5 fm^{-2} from Bernheim *et. al.*). Energy resolution is 0.9 MeV FWHM. Data are unfolded for radiative effects.
2. Threshold experimental data compared to Mathiot's theoretical calculations. The cross sections are averaged over a region of energy loss extending from threshold to a relative CM energy of the np system of 3 MeV. The dotted curve is the impulse approximation, the dash-dotted curve includes π -exchange contribution, the dashed curve includes in addition the ρ -exchange contribution. The solid curve is the total result, in which the Δ -isobar contribution is taken also in account.
3. Threshold deuteron disintegration cross sections by Singh *et. al.* averaged over a 1.5 MeV bin: a) with the Paris potential and b) with the Bonn potential. For each case the calculations are shown for both G_E and F_1 couplings and for the dipole and Gari-Krümpelmann nucleon form-factors. The experimental data are from Saclay ($E_{np} = 0$ to 3 MeV).
4. The Saclay experimental data compared to hybrid quark-hadron model theoretical calculations: a) Best model of Chen and Kisslinger ($r_0=1.0$ fm), b) Best model of Glozman *et. al.* (long-dashed line: IA; short-dashed: includes also six-quark contributions; dot-dashed: includes in addition π -exchange; double-dot-dashed: includes in addition ρ -exchange; solid line: full calculation with inclusion of Δ contribution. Note that the experimental (theoretical) cross sections are averaged over a 3 (1.5) MeV range in E_{np} .

5. The Saclay experimental data compared to the RGM theoretical models:
 - a) Calculations of Yamauchi *et. al.*: the solid and dotted curves are the predictions of the quark cluster theory with and without MEC, whereas the dash-dotted and dash-double-dotted curves those of the conventional model with and without MEC. b) Calculations of Chemtob and Furui: Curve 0 is the impulse approximation, curve 1 is IA with the π -pair term, curve 2 includes also π -currents, curve 3 includes also quark-interchange terms, curve 4 includes also a wave function normalization correction and curves 5, 5', 5'' include the gluon-exchange effects. The latter three curves are for different values of the strong coupling constant. The theoretical cross sections are averaged over a 1.5 MeV energy range.

6. Threshold inelastic cross sections from SLAC experiment NE4 (20 MeV FWHM resolution) averaged over a 10 MeV excitation energy range. The theoretical cross sections of Yamauchi *et. al.* and Arenhovel *et. al.* are averaged also over the same range. For comparison are also shown the 1 MeV FWHM resolution Saclay data. The dotted curve is the expected contribution to the E_{np} range from 0 to 3 MeV from the elastic radiative tail for a 15 cm long liquid deuterium target.

7. The reconstructed elastic peak from the Monte Carlo simulation of the proposed experiment for the highest extreme kinematics of $Q^2 = 100 \text{ fm}^{-2}$ plotted versus the excitation energy: a) including only Landau ionization energy losses, b) including in addition multiple scattering effects, c) full calculation with radiative energy loss included, d) full calculation after correcting for the probable energy loss of the incident electron.

8. Typical expected separation of the elastic peak and the threshold inelastic process ($Q^2 = 70 \text{ fm}^{-2}$). The circles represent the reconstructed elastic peak distribution from the Monte Carlo simulation of the experiment. The dashed curve is the theoretical prediction by Yamauchi *et al.*. The solid curve is a convolution of the theoretical curve with the Monte Carlo resolution function (dotted curve).

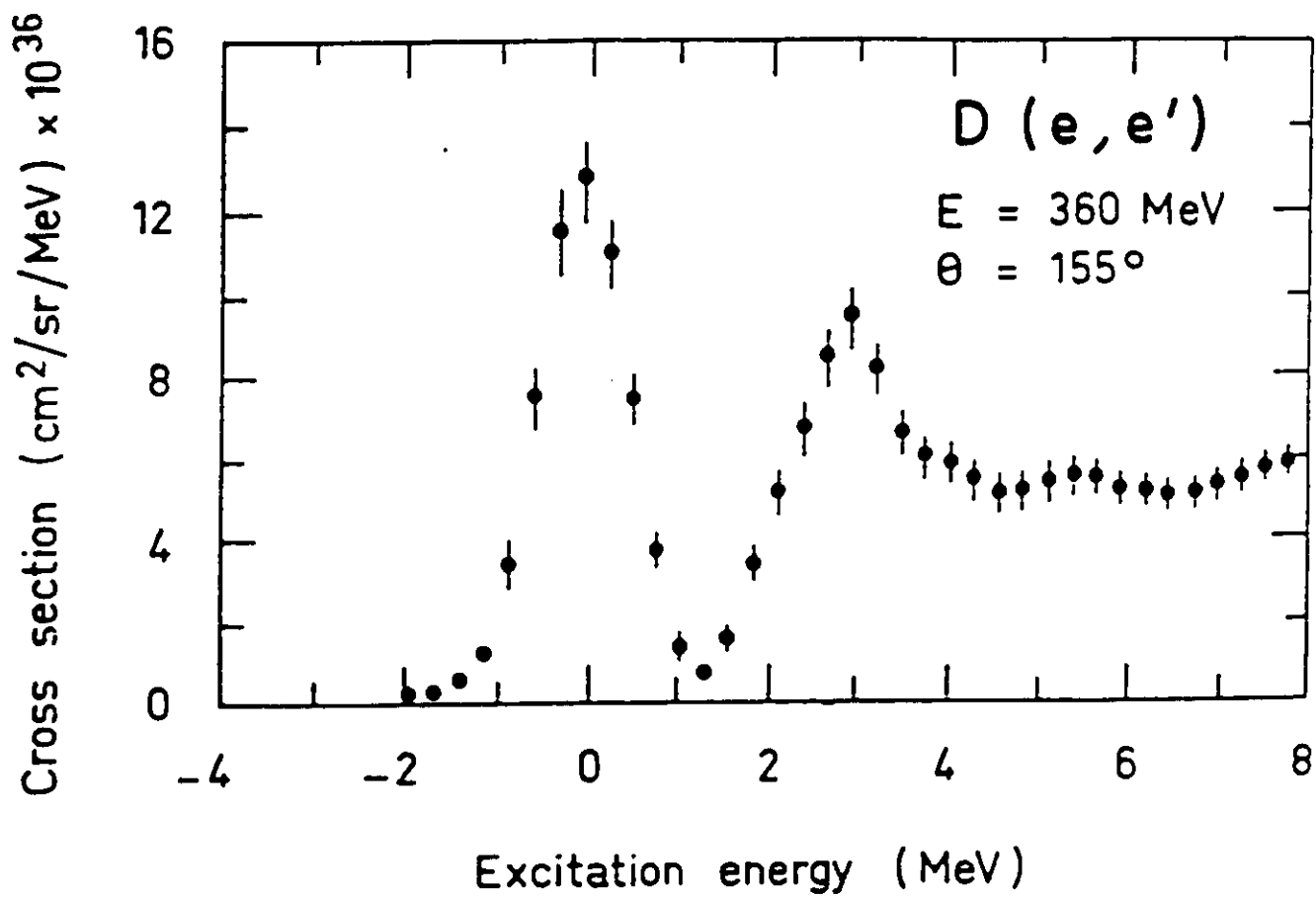


Figure 1

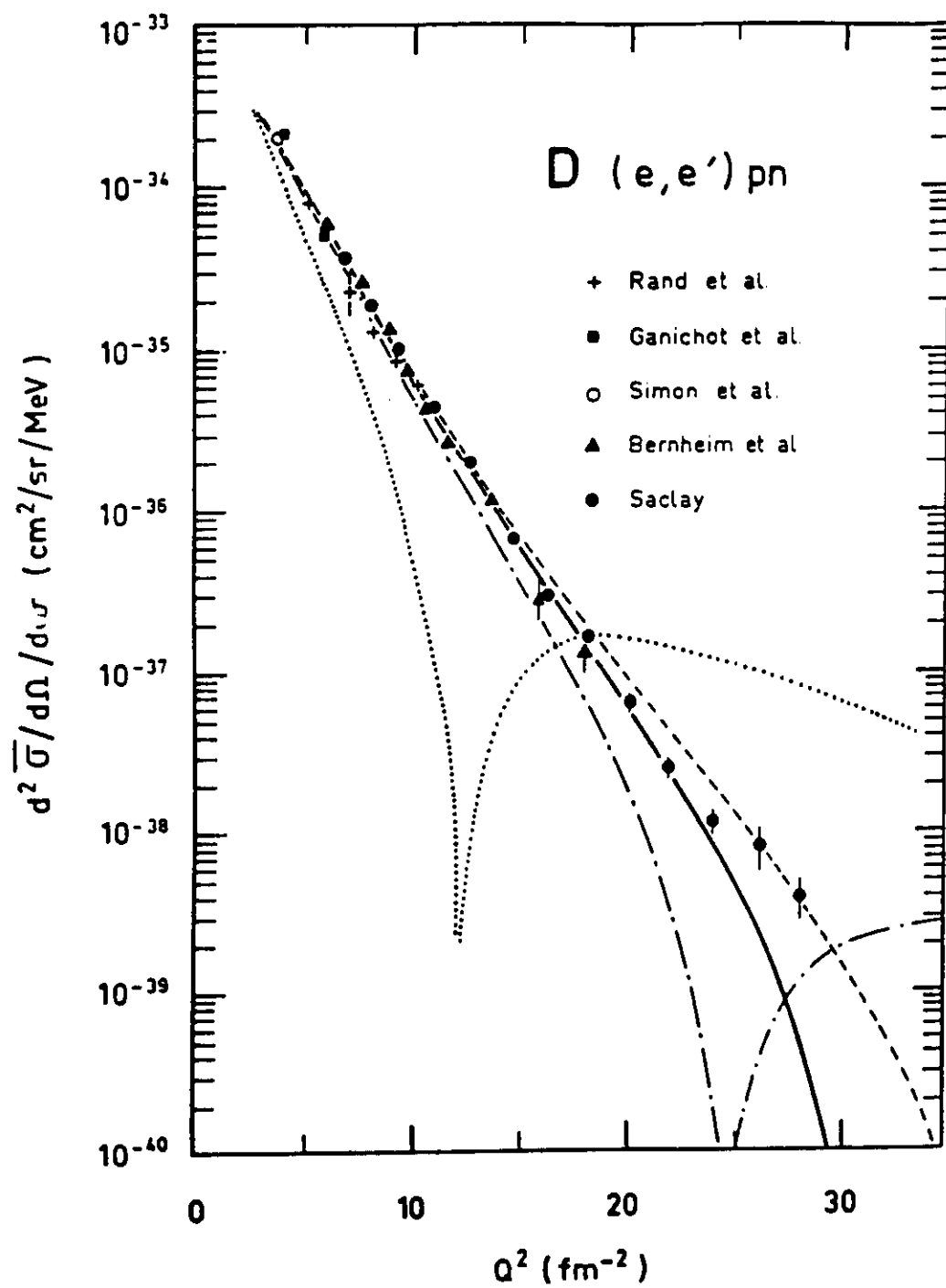


Figure 2

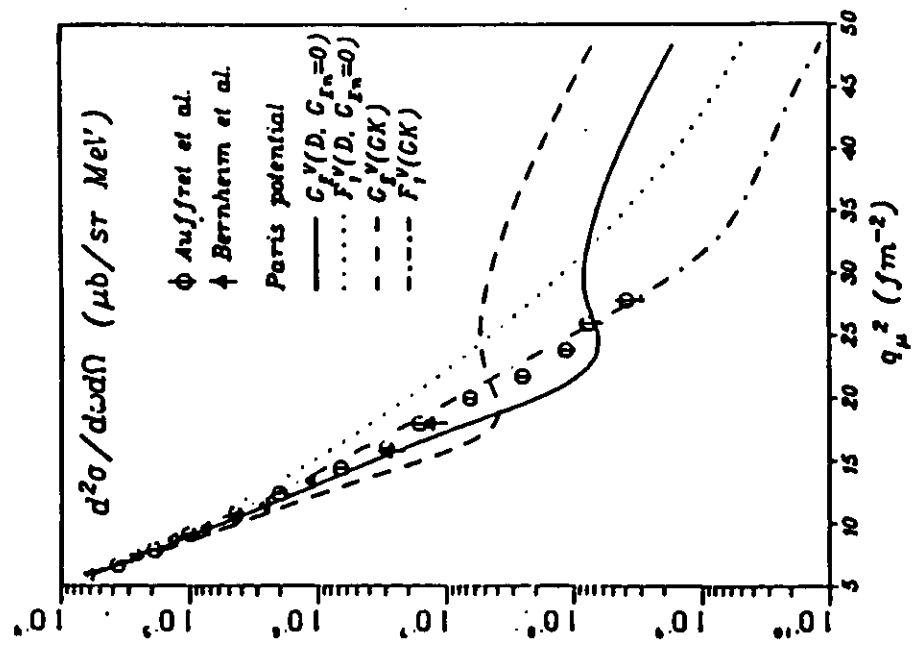


Figure 3-a

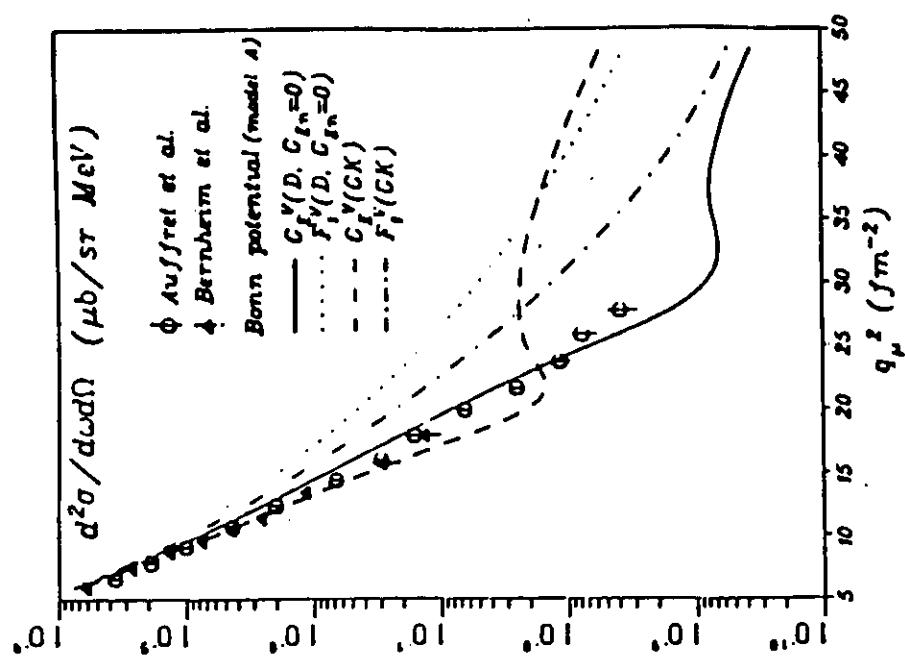


Figure 3-b

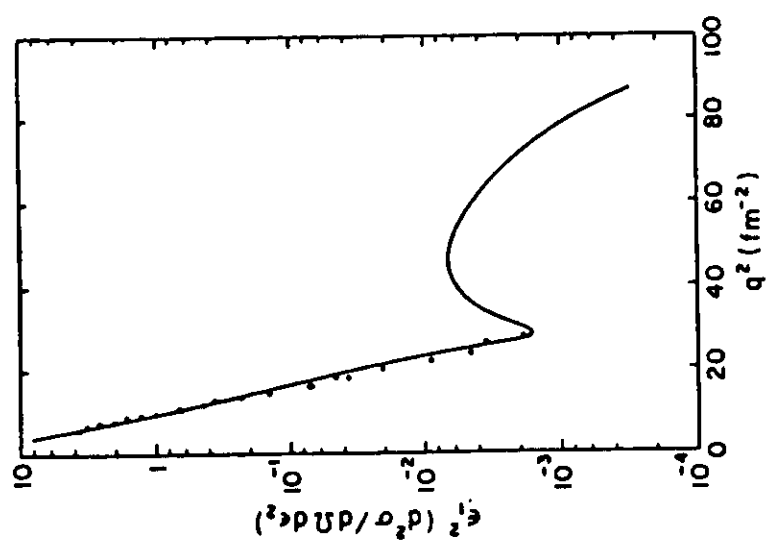


Figure 4-a

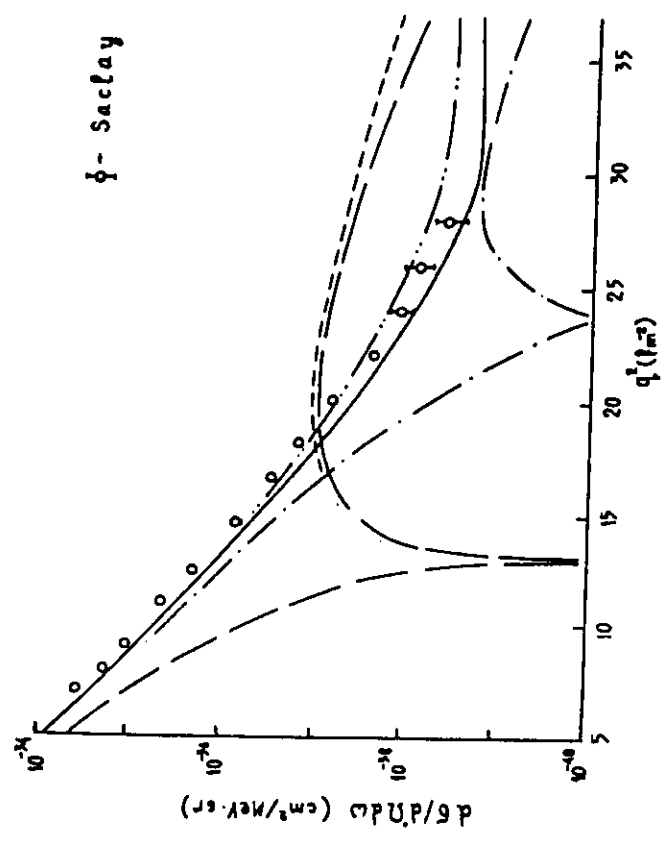


Figure 4-b

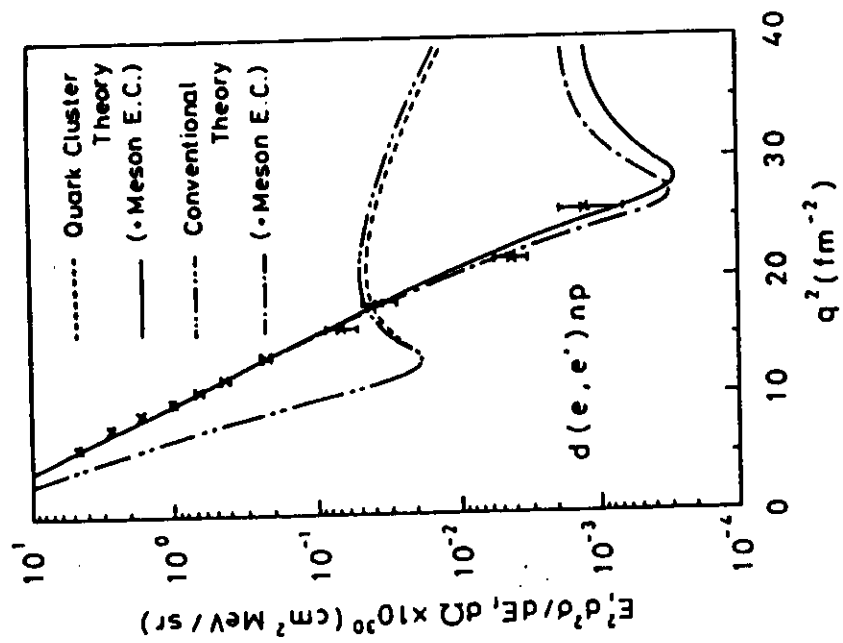


Figure 5-a

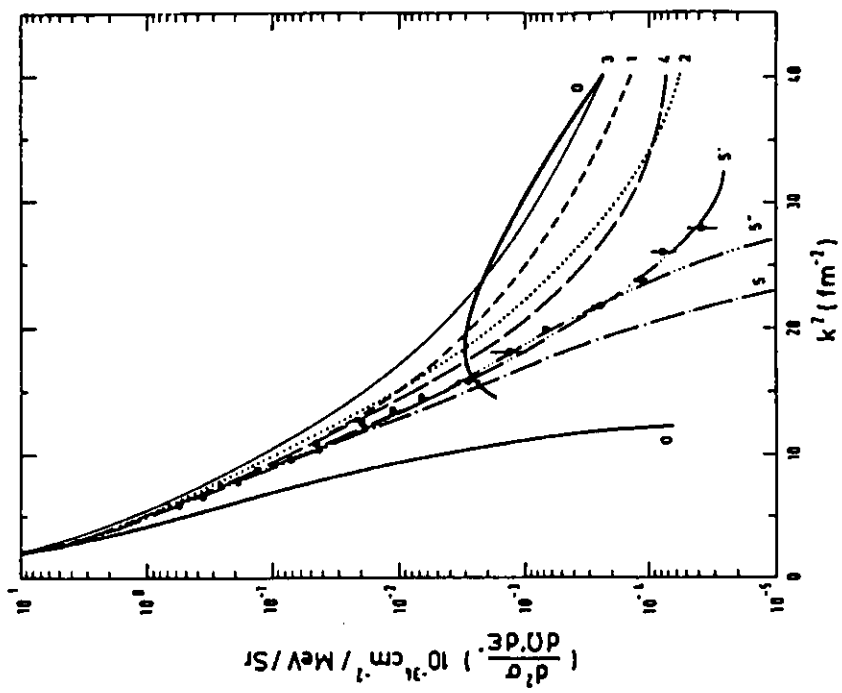


Figure 5-b

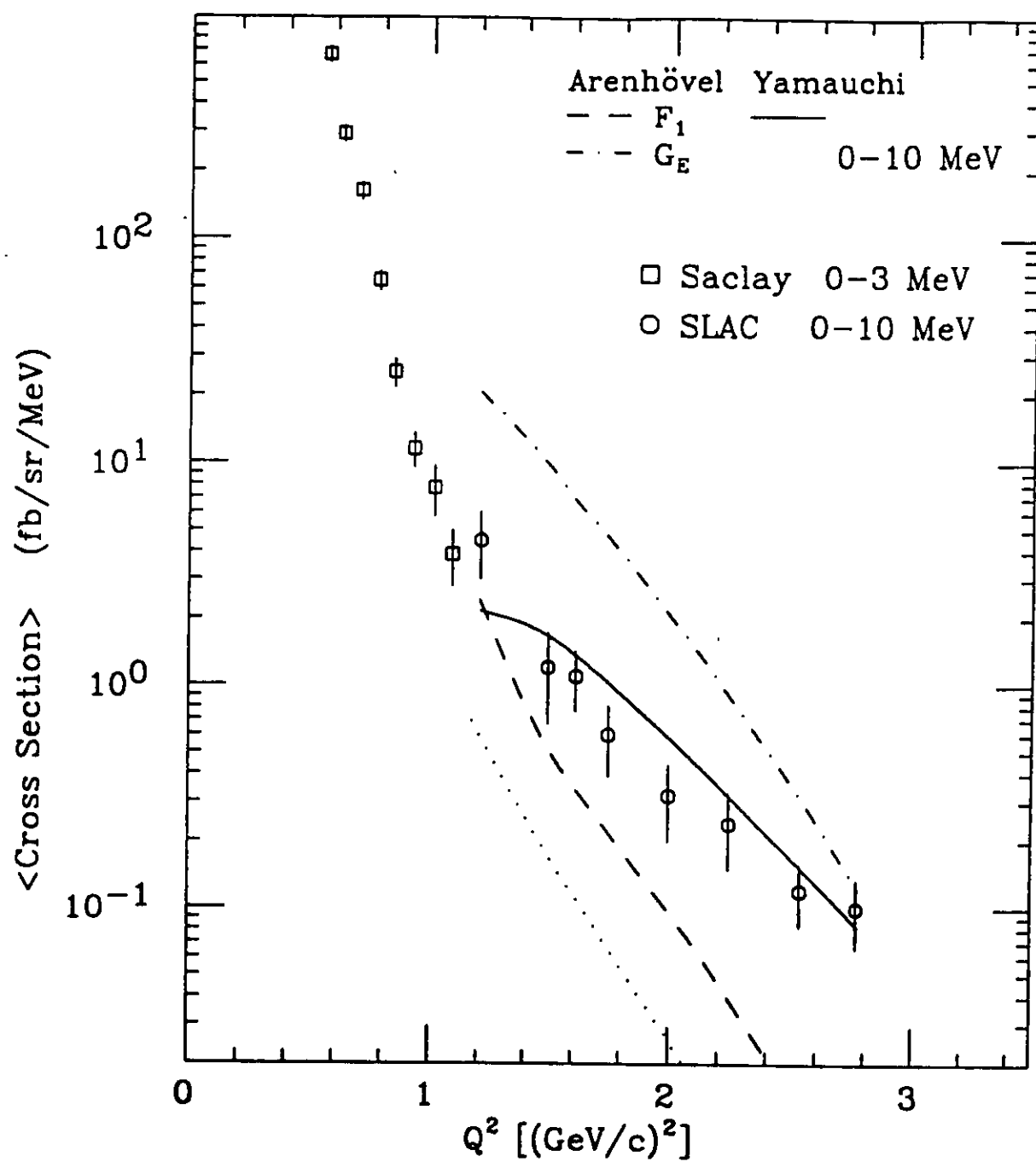


Figure 6

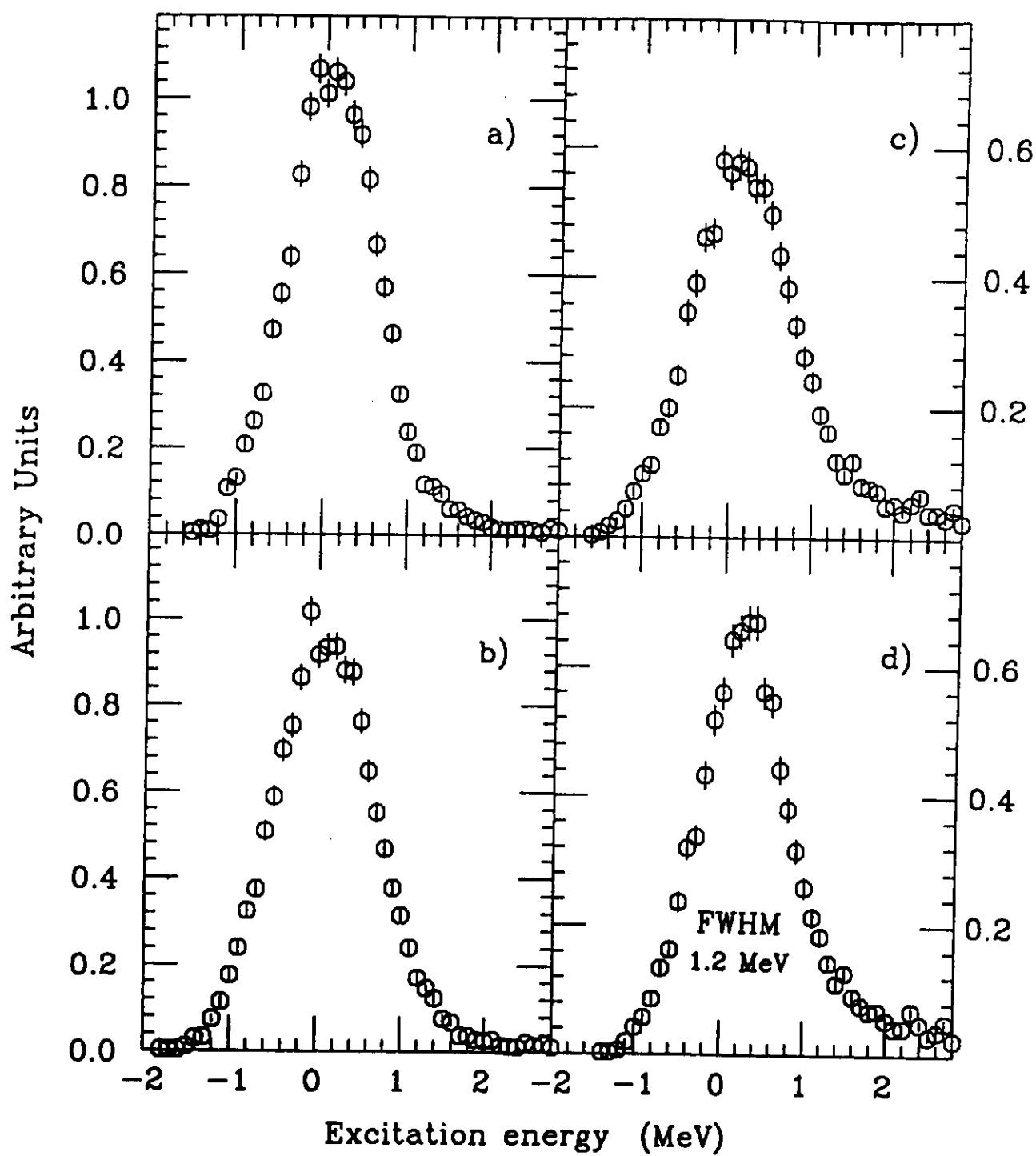


Figure 7

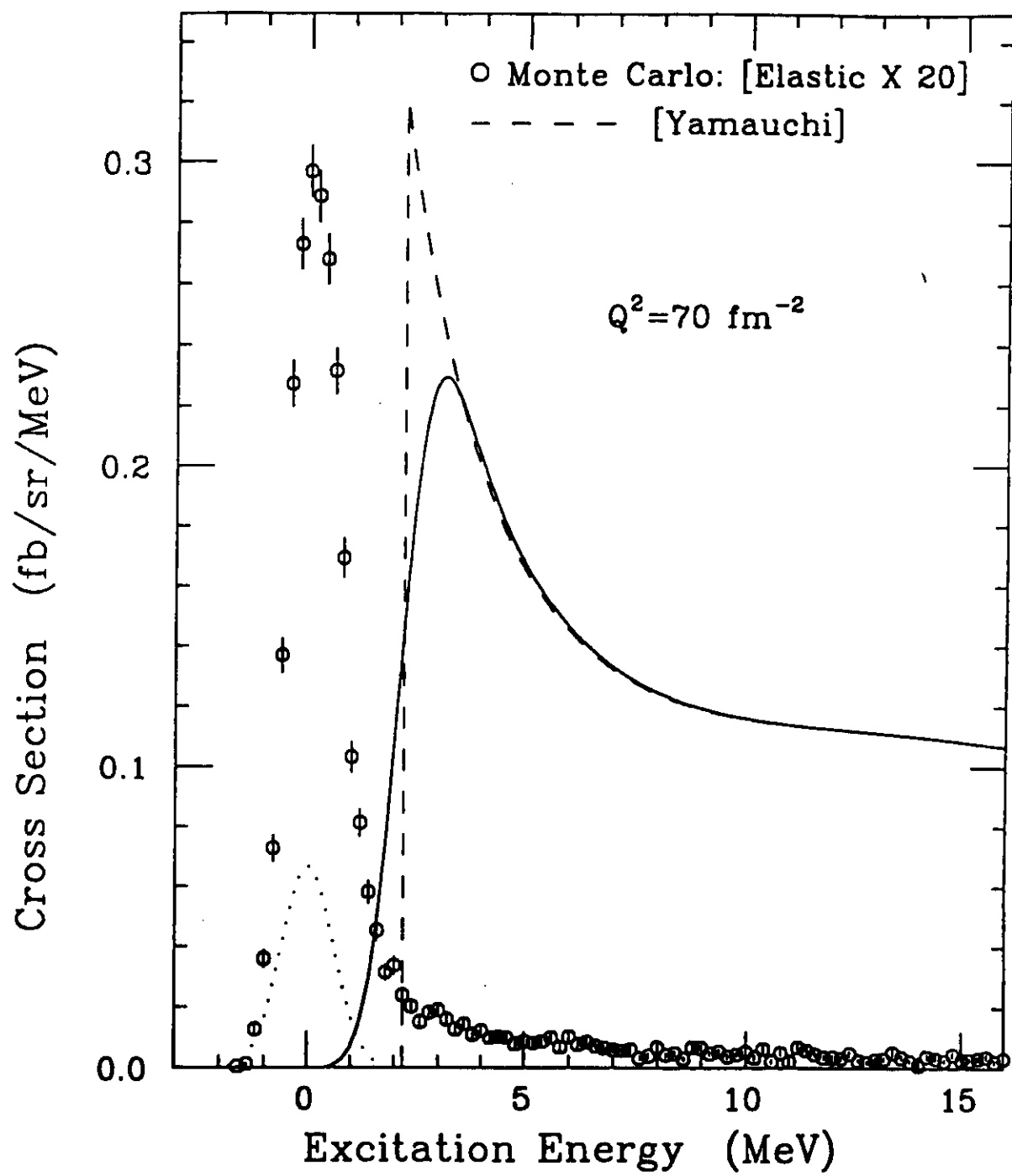


Figure 8